Molecular Basis of Enzyme Inactivation by an Endogenous Electrophile 4-Hydroxy-2-nonenal: Identification of Modification Sites in Glyceraldehyde-3-phosphate Dehydrogenase†

Takeshi Ishii,‡ Emi Tatsuda,‡ Shigenori Kumazawa,§ Tsutomu Nakayama,§ and Koji Uchida*,‡

Laboratory of Food and Biodynamics, Graduate School of Bioagricultural Sciences, Nagoya University, Nagoya 464-8601, Japan, and Laboratory of Functional Food Science, School of Food and Nutritional Sciences, University of Shizuoka, 52-1 Yada, Shizuoka 422-8526, Japan

Received November 13, 2002; Revised Manuscript Received December 26, 2002

ABSTRACT: 4-Hydroxy-2-nonenal (HNE), a major lipid peroxidation-derived reactive aldehyde, is a potent inhibitor of sulfhydryl enzymes, such as the glycolytic enzyme glyceraldehyde-3-phosphate dehydrogenase (GAPDH). It has been suggested that HNE exerts an inhibitory effect on the enzyme due to the modification of the cysteine residue (Cys-149) at the catalytic site generating the HNE−cysteine Michael addition-type adduct [Uchida, K., and Stadtman, E. R. (1993) *J. Biol. Chem. 268*, 6388−6393]. In the study presented here, to elucidate the mechanism for the inactivation of GAPDH by HNE, we attempted to identify the modification sites of the enzyme by monitoring the formation of the HNE Michael adducts by mass spectrometric methods. Incubation of GAPDH (1 mg/mL) with 1 mM HNE in 50 mM sodium phosphate buffer (pH 7.4) at 37 °C resulted in a time-dependent loss of enzyme activity, which was associated with the covalent binding of HNE to the enzyme. To identify the site of modification of GAPDH by HNE, both the HNE-pretreated and untreated GAPDH were digested with trypsin and V8 protease, and the resulting peptides were subjected to electrospray ionization liquid chromatography−mass spectrometry (ESI-LC−MS). This technique identified five peptides, which contained the HNE adducts at His-164, Cys-244, Cys-281, His-327, and Lys-331 and revealed that both His-164 and Cys-281 were very rapidly modified at 5 min, followed by Cys-244 at 15 min and His-327 and Lys-331 at 30 min. These observations and the observation that the HNE modification of the catalytic center, Cys-149, was not observed suggest that the HNE inactivation of GAPDH is not due to the modification of the catalytic center but to the selective modification of amino acids primarily located in the surface of the GAPDH molecule.

Several lines of evidence indicate that the oxidative modification of a protein and the subsequent accumulation of the modified proteins have been found in cells during aging, oxidative stress, and in various pathological states, including premature diseases, muscular dystrophy, rheumatoid arthritis, and atherosclerosis (*1*, *2*). The important agents that give rise to the modification of a protein may be represented by reactive aldehydic intermediates, such as keto aldehydes, 2-alkenals, and 4-hydroxy-2-alkenals (*3*, *4*). These reactive aldehydes are considered important mediators of cell damage due to their ability to covalently modify biomolecules, which can disrupt important cellular functions and can cause mutations (*3*). Furthermore, the adduction of aldehydes to apolipoprotein B in low-density lipoproteins (LDLs) has been strongly implicated in the mechanism by which LDL is converted to an atherogenic form that is taken up by macrophages, leading to the formation of foam cells (*5*, *6*). 4-Hydroxy-2-nonenal (HNE),[1] among the reactive aldehydes, is a major product of lipid peroxidation (*3*, *7*, *8*) and is believed to be largely responsible for the cytopathological effects observed during oxidative stress (*3*). HNE exerts these effects because of its facile reactivity with biological materials, particularly sulfhydryl groups of proteins (*9*). The reaction of HNE with sulfhydryl groups leads to the formation of thioether adducts that further undergo cyclization to form cyclic hemiacetals (*3*, *10*). The formation of thiol-derived Michael adducts, stabilized as cyclic hemiacetals, was initially considered to constitute the main reactivity of HNE (*3*). However, other studies led to the realization that HNE could also form Michael adducts with the imidazole moiety of the histidine residues (*11*) and the ϵ-amino group of the lysine residues (*12*) (Figure 1).

Glyceraldehyde-3-phosphate dehydrogenase (GAPDH), a key enzyme in intermediary metabolism, is highly sensitive

† This work was supported by a research grant from the Ministry of Education, Culture, Sports, Science, and Technology and by the COE Program in the 21st Century in Japan.

* To whom correspondence should be addressed: Laboratory of Food and Biodynamics, Graduate School of Bioagricultural Sciences, Nagoya University, Nagoya 464-8601, Japan. Telephone: 81-52-789-4127. Fax: 81-52-789-5741. E-mail: uchidak@agr.nagoya-u.ac.jp.

‡ Nagoya University.

§ University of Shizuoka.

[1] Abbreviations: HNE, 4-hydroxy-2-nonenal; GAPDH, glyceraldehyde-3-phosphate dehydrogenase; DNPH, 2,4-dinitrophenylhydrazine; MALDI-TOF MS, matrix-assisted laser desorption and ionization time-of-flight mass spectrometry; ESI-LC−MS, electrospray ionization liquid chromatography−mass spectrometry; ESI-LC−MS/MS, electrospray ionization liquid chromatography−mass spectrometry/mass spectrometry.

10.1021/bi027172o CCC: $25.00
Published on Web 03/08/2003

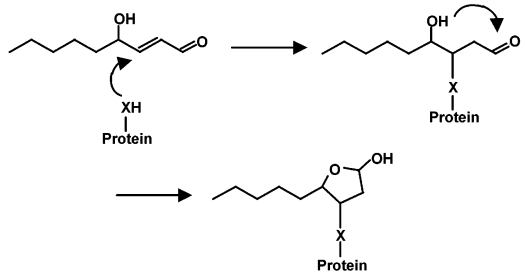

FIGURE 1: Formation of Michael addition-type HNE−amino acid adducts. HNE forms Michael adducts with cysteine, histidine, and lysine residues of the protein. X represents the sulfhydryl group of cysteine, the imidazole group of histidine, and the ϵ-amino group of the lysine residues.

to inactivation by lipid peroxidation products *in vitro* and *in vivo* (*13*−*16*). In addition, a previous study has shown that the HNE treatment of cultured kidney cells results in the formation of the HNE-modified GAPDH (*17*). The high sensitivity of GAPDH to inactivation by lipid peroxidation products, such as HNE, has been attributed to the modification of Cys-149, which is at the catalytic site of the enzyme. However, this theory has not yet been proved. Thus, to gain a better understanding of the molecular basis of the HNE inactivation of GAPDH, we attempted to identify the HNE modification sites of the enzyme using mass spectrometric procedures.

EXPERIMENTAL PROCEDURES

Materials. The stock solution of *trans*-4-hydroxy-2-nonenal was prepared by the acid treatment (1 mM HCl) of HNE diethylacetal, which was synthesized according to the procedure of De Montarby *et al*. (*18*). The concentration of the HNE stock solution was determined by measurement of the UV absorbance at 224 nm. Rabbit muscle GAPDH (10 mg/mL) suspended in a 3.2 M ammonium sulfate solution (pH 7.5) containing 0.1 mM EDTA was obtained from Rosche Diagnostics (Mannheim, Germany). The anti-HNE−histidine monoclonal antibody (mAbHNEJ2) was kindly provided by the Nihon Oil Factory (NOF) Co. (Tokyo, Japan) (*19*). The horseradish peroxidase-linked anti-rabbit IgG immunoglobulin and ECL (enhanced chemiluminescence) Western blotting detection reagents were obtained from Amersham Pharmacia Biotech (Buckinghamshire, U.K.). Sequence-grade modified trypsin was purchased from Promega Corp. *Staphylococcus aureus* V8 protease (endoproteinase Glu-C) was purchased from Wako Pure Chemical Industries, Ltd. (Osaka, Japan).

Reaction of GAPDH with HNE. The GAPDH solution (2 mg/mL) was prepared by dilution of the enzyme suspension with 50 mM sodium phosphate buffer (pH 7.4). An aliquot (0.5 mL) of the enzyme solution was mixed with an equal volume of an HNE solution (2 mM) and incubated at 37 °C. The reaction was stopped by the addition of 100 μL of 10 mM *N*-acetylcysteine. For determination of the GAPDH activity, a 10 μL aliquot of the reaction mixture was assayed in 3 mL of 15 mM sodium pyrophosphate and 30 mM sodium arsenate buffer (pH 8.5). The reaction of GAPDH was initiated by the addition of 100 μL of 7.5 mM NAD, 100 μL of 0.1 mM dithiothreitol, and 100 μL of 15 mM DL-glyceraldehyde 3-phosphate. The mixture was incubated at room temparature for 5 min, and the absorbance at 340 nm was measured.

Protein Carbonyl. An aliquot (0.5 mL) of the protein samples was treated with an equal volume of 0.1% (w/v) 2,4-dinitrophenylhydrazine (DNPH) in 2 N HCl and incubated for 1 h at room temperature. This mixture was treated with 0.5 mL of 20% trichloroacetic acid (w/v, final concentration), and after centrifugation, the precipitate was extracted three times with ethanol and ethyl acetate (1:1, v/v). The protein sample was then dissolved with 2 mL of 8 M guanidine hydrochloride, 13 mM EDTA, and 133 mM Tris solution (pH 7.4), and the UV absorbance was measured at 365 nm. The results were expressed as moles of DNPH incorporated per mole of protein based on an average absorptivity of 21.0 mM^{-1} cm^{-1} (*20*).

Amino Acid Analysis. An aliquot (0.1 mL) of the protein samples incubated in the absence or presence of crotonaldehyde was treated with 10 mM EDTA (10 μL), 1 N NaOH (10 μL), and 100 mM $NaBH_4$ (10 μL). After incubation for 1 h at 37 °C, the mixture was treated with 10% trichloroacetic acid. After centrifugation at 10000*g* for 3 min, the proteins were hydrolyzed *in vacuo* with 6 N HCl for 24 h at 105 °C. The hydrolysates were then concentrated and dissolved in 50 mM sodium phosphate buffer (pH 7.4). The amino acid analysis was performed using a JEOL JLC-500 amino acid analyzer equipped with a JEOL LC30-DK20 data analyzing system.

SDS−Polyacrylamide Gel Electrophoresis (SDS−PAGE). SDS−polyacrylamide gel electrophoresis (SDS−PAGE) was performed according to the method of Laemmli (*21*). The protein was stained with Coomassie blue.

Immunoblot Analysis. A gel was transblotted onto a nitrocellulose membrane, incubated with Block Ace (40 mg/mL) for blocking, washed, and treated with the primary antibody. This procedure was followed by the addition of horseradish peroxidase conjugated to a goat anti-mouse IgG $F(ab')_2$ fragment and ECL reagents (Amersham Pharmacia Biotech). The bands were visualized by exposure of the membranes to autoradiography film.

Electrospray Ionization Liquid Chromatography−Mass Spectrometry/Mass Spectrometry (ESI-LC−MS/MS) Analysis. The ESI-LC−MS/MS analyses were performed on an LCQ ion trap mass system (ThermoQuest) equipped with an electrospray ion source. The electrospray system employed a spray voltage of 5 kV and a capillary temperature of 260 °C.

Matrix-Assisted Laser Desorption and Ionization Time-of-Flight Mass Spectrometry (MALDI-TOF MS). Native and HNE-modified GAPDH were mixed with a saturated solution of 3,5-dimethoxy-4-hydroxycinnamic acid containing 75% acetonitrile and 0.1% trifluoroacetic acid and dried on stainless steel targets at room temperature and pressure. The analyses were performed using a Voyager matrix-assisted laser desorption and ionization time-of-flight mass spectrometer (Applied Biosystems Japan, Ltd., Tokyo, Japan) with a nitrogen laser (337 nm). All analyses were carried out in the positive ion mode, and the instrument was calibrated immediately prior to each series of studies.

Peptide Mapping. The native and HNE-modified GAPDHs (0.3 mg/mL) were digested with modified with trypsin in 0.25 mL of 50 mM sodium phosphate buffer (pH 8.0) at 37 °C for 24 h using an enzyme:substrate ratio of 1:100 (w/w). After the pH of the phosphate buffer had been adjusted by adding acetic acid, at pH 7.4, the samples were further

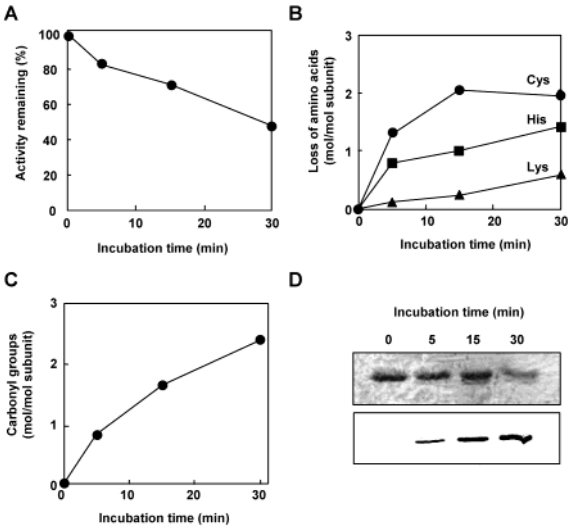

FIGURE 2: Covalent attachment of HNE to protein. BSA (1 mg/mL) was incubated with 0−1 mM HNE in 50 mM sodium phosphate buffer (pH 7.4) at 37 °C. (A) Changes in GAPDH activity. (B) Loss of amino acid residues. An aliquot (0.1 mL) was taken from the reaction mixture, and the amount of amino acids was determined by amino acid analysis as described in Experimental Procedures: cysteine (●), histidine (■), and lysine residues (▲). (C) Introduction of carbonyl groups into protein upon reaction with crotonaldehyde. The protein carbonyl content was determined by the procedure using DNPH. (D) SDS−PAGE (top) and immunoblot (bottom) analyses of the HNE−histidine Michael adduct with mAbHNEJ2.

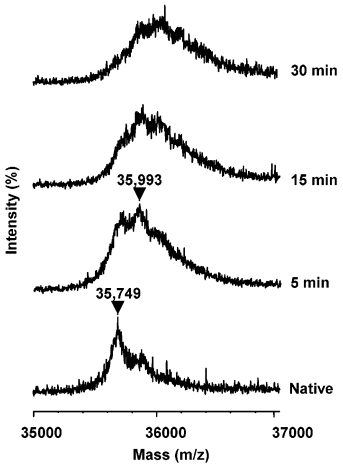

FIGURE 3: MALDI-TOF MS analysis of HNE-treated GAPDH. The HNE-treated GAPDH was prepared upon incubation of GAPDH (0.1 mg/mL) with 1 mM HNE in 0.1 M sodium phosphate buffer (pH 7.4) at 37 °C. A second higher-mass peak of native GAPDH may represent a matrix adduct.

digested with V8 protease at 37 °C for 24 h using an enzyme:substrate ratio of 1:50 (w/w). Peptide samples were analyzed by a reversed-phase HPLC system, which consisted of a nanospace SI-1 HPLC system (SHISEIDO Co., Ltd., Tokyo, Japan) with a FP-1520 fluorescence detector (Jasco Co., Tokyo, Japan), using a Capcell Pak C18 UG120 column [2.0 mm × 250 mm (inside diameter), Shiseido, Japan]. These samples were eluted with a linear gradient of water containing 0.1% formic acid (solvent A) and acetonitrile containing 0.08% formic acid (solvent B) (10% B from 0 to 5 min and 55% B from 5 to 80 min). The flow rate was 0.2 mL/min, and the column temperature was controlled at 40 °C. The chromatograms were recorded at 215 nm.

Three-Dimensional Structure of GAPDH. The structure was drawn using swis-PdbViewer version 3.7b2 (ExPASy Molecular Biology Server), and the PDB coordinates for rabbit GAPDH (AAAa0LY2A) were obtained from an automated comparative protein modeling server (SWISS-MODEL in ExPASy Molecular Biology Server).

RESULTS

Covalent Binding of HNE to GAPDH. We first examined the correlation between the enzyme inactivation and covalent binding of HNE to GAPDH during 30 min of incubation. As shown in Figure 2A, upon incubation of GAPDH (1 mg/mL) with 1 mM HNE in 50 mM sodium phosphate buffer (pH 7.4) at 37 °C, the enzyme activity linearly decreased to 50% of the initial value after 30 min. To evaluate the binding of HNE to the enzyme, we examined changes in the amino acid composition, the generation of the protein-linked carbonyl groups, and the increase in the immunoreactivity with an anti-HNE−histidine monoclonal antibody. As shown in Figure 2B, the exposure of GAPDH to HNE resulted in the selective loss of cysteine, histidine, and lysine residues, and approximately 2 molecules of cysteine, 1.4 molecules of histidine, and 0.6 molecule of lysine residues per subunit were lost after 30 min. In addition, the loss of the amino acids was accompanied by a time-dependent increase in the extent of protein carbonyl formation, and approximately 2.3 molecules of carbonyl groups per subunit were newly generated in the protein after 30 min (Figure 2C). The results depicted in panels B and C of Figure 2 suggest that at least 60% of the HNE bound to the amino acids (cysteine, histidine, and lysine) constitute the Michael adducts which possess a carbonyl functionality. Moreover, consistent with the loss of histidine residues in the enzyme, a time-dependent increase in the immunoreactivity with the anti-HNE−histidine monoclonal antibody (mAbHNEJ2) was observed (Figure 2D).

To further examine the covalent binding of HNE to the enzyme, the native and the HNE-treated GAPDH for 5−30 min were analyzed by MALDI-TOF MS. As shown in Figure 3, the analysis of the native GAPDH revealed a peak at *m*/*z* 35.699. When GAPDH was incubated with 1 mM HNE in 50 mM sodium phosphate buffer (pH 7.4) for 5 min at 37 °C, some unmodified GAPDH subunits were observed (*m*/*z* 35.749) as well as the peak (*m*/*z* 35.993) corresponding to the addition of one to two molecules of HNE per subunit. Further incubations resulted in the appearance of peaks corresponding to the addition of one to three molecules of HNE. The sequential peaks in the spectrum of the HNE−GAPDH complex all differed in molecular mass by ~160 Da, which was close to the molecular mass of HNE (156 Da). This increase in the molecular mass provided strong evidence that the reaction between HNE and GAPDH primarily occurred *via* the Michael addition reaction.

Peptide Mass Mapping by ESI-LC−MS Analysis. To characterize the structural modification of GAPDH by HNE, the native and HNE-treated GAPDHs were digested with trypsin and V8 protease and then analyzed by ESI-LC−MS. Peptide mass mapping by ESI-LC−MS analysis of the peptides from the native GAPDH provided identification of the peptides accounting for approximately 70% of the protein sequence (Figure 4 and Table 1). Relative to the calculated

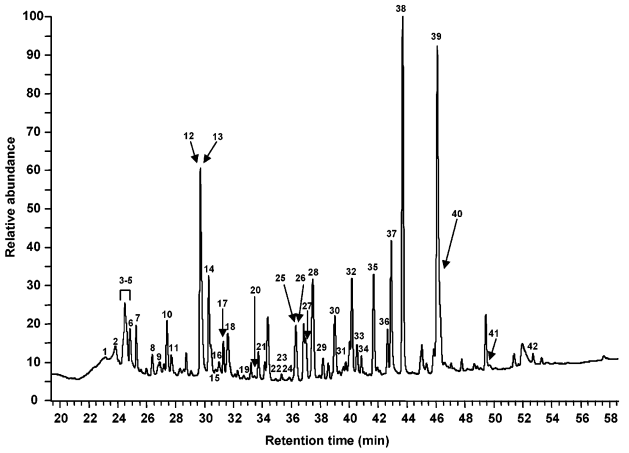

FIGURE 4: ESI-LC−MS analysis of peptides from GAPDH digested with trypsin and V8 protease. Purified rabbit muscle GAPDH was digested with trypsin and V8 protease, and ESI-LC−MS was performed with an LCQ ion trap mass spectrometer as described in Experimental Procedures. The elution positions of the identified tryptic peptides are indicated in the total ion current and summarized in Table 1.

Table 1: Peptides Identified by ESI-LC−MS from Native GAPDH

sequence positions	molecular mass (Da)	sequence	peak no.
3−10	805.9	VGVNGFGR	23
14−17	488.2	LVTR	1
18−24	694.2	AAFNSGK	3
25−36	1316.2	VDVVAINDPFID	40
53−58	688.1	FHGTVK	2
61−69	940.4	NGKLVINGK	21
64−69	643.2	LVINGK	15
70−76	821	AITIFQE	38
70−77	977.3	AITIFQER	32
77−83	812.2	RDPANIK	22
78−83	657.1	DPANIK	7
84−94	1194.2	WGDAGAEYVVE	34
95−103	972	STGVFTTME	36
95−104	1100.3	STGVFTTMEK	27
95−104	1116.2	STGVFTT#MEK	19
105−114	907.3	AGAHLKGGAK	24
116−124	913.4	VIISAPSXD	25
136−142	867.3	KYDNSLK	6
137−142	739.1	YDNSLK	9
143−159	1703.5	IVSNASCTTNCLAPLAK	31
160−169	1165.3	VIHDHFGIVE	28
170−183	1800.9	GL#MTTVHAITATQKTVD	33
192−194	474.1	LWR	12
198−212	1369.4	GAAQNIIPASTGAAK	26
232−241	1026.4	VPTPNVSVVD	35
242−247	732.1	LTCRLE	4
246−251	660.9	LEKAAK	39
252−256	653.1	YDDIK	8
252−257	781.1	YDDIKK	5
258−264	758.1	VVKQASE	20
261−268	829.1	QASEGPLK	10
265−276	1260.3	GPLKGILGYTED	16
269−275	752	GILGYTE	37
269−282	1496.5	GILGYTEDQVVSCD	11
277−282	764.2	DQVVSCD	13
294−302	1312.4	AGAGIALND	29
315−320	743.2	FGYSNR	14
321−332	1358.4	VVDLMVHMASKE	30
324−331	916.2	LMVHMASK	17
324−332	1045.2	LMVHMASKE	18

masses of the unmodified peptides, three peptides, which showed an increased mass of 156 Da corresponding to the addition of a single molecule of HNE, were detected by ESI-LC−MS analysis, namely, **p-1** (His-Phe-Gly-Ile-Val-Glu),

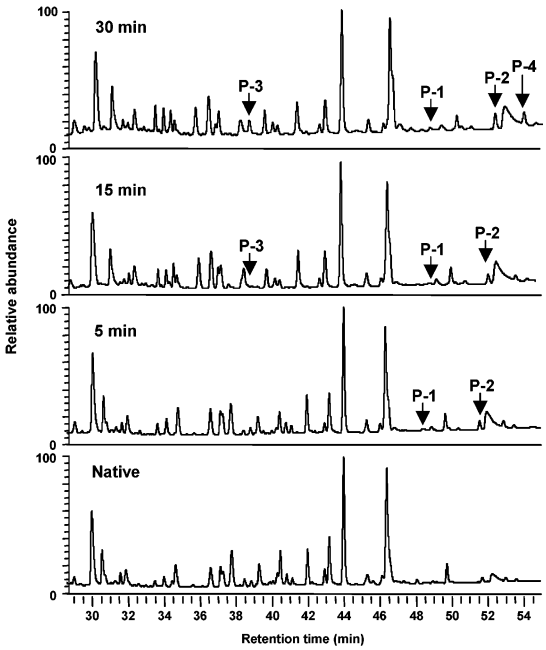

FIGURE 5: ESI-LC−MS analysis of peptides from HNE-modified GAPDH digested with trypsin and V8 protease. Purified rabbit muscle GAPDH was modified with HNE, digested with trypsin and V8 protease, and analyzed by ESI-LC−MS.

p-2 (Asp-Gln-Val-Val-Ser-Cys-Asp), and **p-3** (Leu-Thr-Cys-Arg) (Figure 5). Furthermore, we also detected one peptide, **p-4** (Leu-Met-Val-His-Met-Ala-Ser-Lys), which had an increase in mass of 312 Da corresponding to the addition of two HNE Michael adducts. Peptides **p-1** and **p-2** most rapidly appeared at 5 min, followed by peptide **p-3** at 15 min and peptide **p-4** at 30 min. These peptides were also detected without the HNE Michael adducts, indicating that the 30 min HNE treatment did not yield quantitative modifications of the intact protein. No other peptides with Michael adducts were observed by ESI-LC−MS. These data strongly suggest that possible HNE modification sites in these peptides represent the histidine residue of **p-1**, the cysteine residues of **p-2** and **p-3**, and the histidine and lysine residues of **p-4**.

Identification of HNE Modification Sites by ESI-LC−MS/MS Analysis. To confirm the HNE modification sites, the HNE-modified fragments (**p-1**−**p-4**) were further analyzed by ESI-LC−MS/MS without additional chromatography. The MS/MS spectrum of the $[M + H]^+$ ion at *m*/*z* 857.5 from the HNE-modified fragment (**p-1**) with the sequence His-Phe-Gly-Ile-Val-Glu is shown in Figure 6A. In the MS/MS analysis, the singly charged C-terminal product ion (y_2) and its H_2O loss ion (y_{3-18}) were observed. The masses of the N-terminal fragment ions (b_1−b_5 and a-series ions) and the H_2O or NH_3 loss fragment ions (b_{2-18}, b_{3-18}, b_{4-18}, and a_{3-17}) were observed to increase 156 Da, suggesting that the HNE modification site in the sequence is on His-164. The MS/MS spectrum of the $[M + H]^+$ ion at *m*/*z* 919.4 from the HNE-modified fragment (**p-2**) with the sequence Asp-Gln-Val-Val-Ser-Cys-Asp is shown in Figure 6B. The singly charged N-terminal product ions (b_5) and the H_2O loss product ion (b_{5-18}) were observed in the MS/MS analysis. The masses of the fragment ions (y_2, y_4−y_6, and b_6) and the NH_3 loss fragment ions (y_{2-17} and b_{6-17}) were observed to increase 156 Da. These results suggest that the HNE Michael adduct is associated with Cys-281. Figure 6C shows the MS/

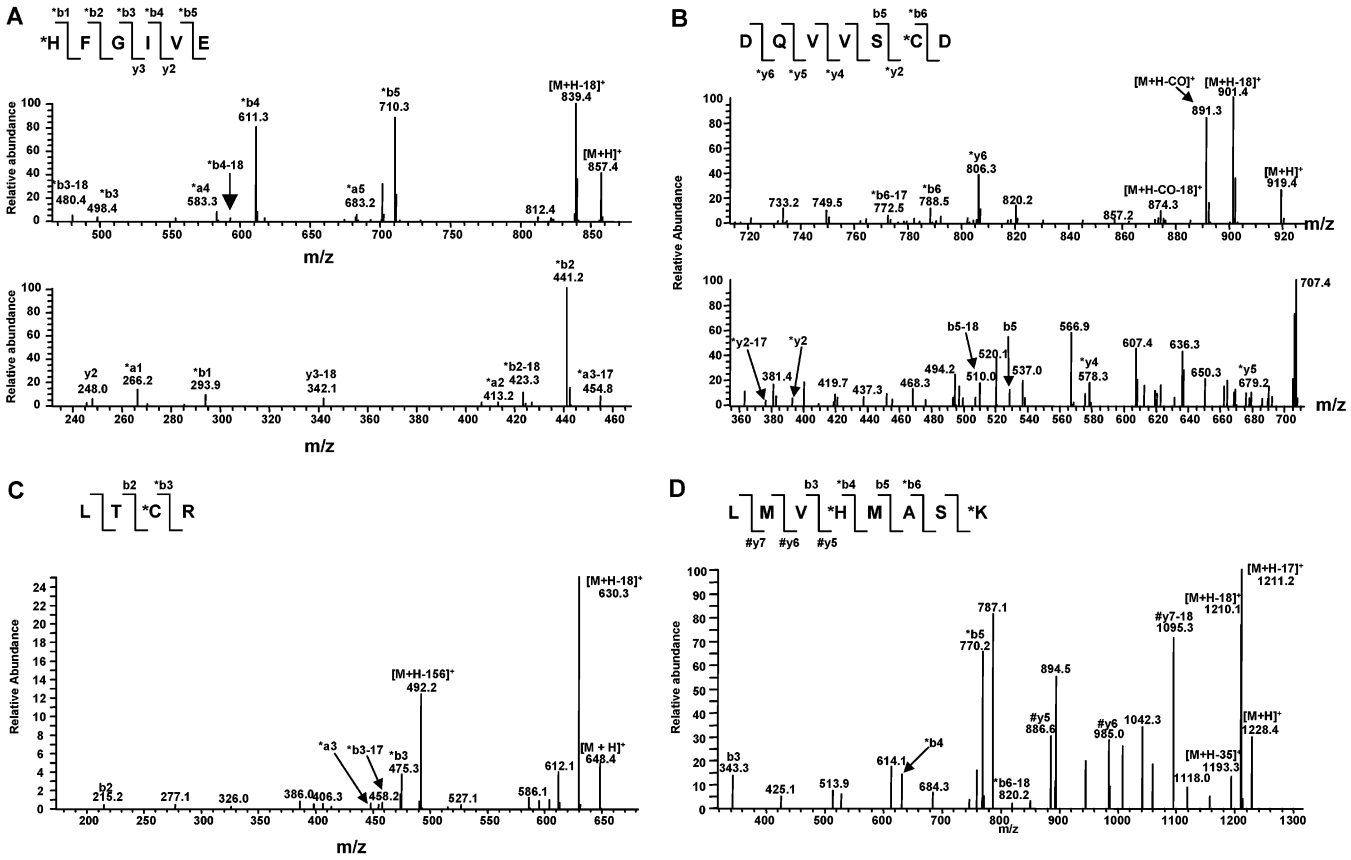

FIGURE 6: ESI-LC−MS/MS spectra of the HNE-modified peptides. (A) Nanoelectrospray MS/MS spectrum of the $[M + H]^+$ ion at *m/z* 857.5 from the HNE-modified fragment (**p-1**) with the sequence His-Phe-Gly-Ile-Val-Glu. (B) Nanoelectrospray MS/MS spectrum of the $[M + H]^+$ ion at *m/z* 919.4 from the HNE-modified fragment (**p-2**) with the sequence Asp-Gln-Val-Val-Ser-Cys-Asp. (C) Nanoelectrospray MS/MS spectrum of the $[M + H]^+$ ion at *m/z* 648.4 from the HNE-modified fragment (**p-3**) with the sequence Leu-Thr-Cys-Arg. (D) Nanoelectrospray MS/MS spectrum of the $[M + H]^+$ion at *m/z* 1228.4 (**p-4**) with the sequence Leu-Met-Val-His-Met-Ala-Ser-Lys.

MS spectrum of the $[M + H]^+$ ion at *m/z* 648.4 from the HNE-modified fragment (**p-3**) with the sequence Leu-Thr-Cys-Arg. One singly charged product ion (b_2) was observed in the MS/MS analysis. The masses of fragment ions (b_3 and a_3) and NH_3 loss fragment ions (b_{3-17}) were observed to increase 156 Da. In addition, a neutral loss ion ($[M + H - 156]^+$) was also observed. These results confirmed that the HNE Michael adduct is on Cys-281. Figure 6D shows the MS/MS spectrum of the $[M + H]^+$ ion at *m/z* 1228.4 (**p-4**) with the sequence Leu-Met-Val-His-Met-Ala-Ser-Lys plus the mass addition of 312 Da. In the MS/MS analysis, one single charged product ion (b_3) was observed. The masses of several fragment (y_5 and y_6) and H_2O loss fragment ions (y_{7-18}) were also observed to increase 312 Da. In addition, the masses of several fragment ions (b_5) and H_2O loss fragment ions (y_{6-18}) were observed to increase 156 Da. These data indicated that His-327 and Lys-331 represented the HNE modification sites due to the 312 Da increase in the mass value. Thus, we identified the five target amino acids of the HNE modification in GAPDH. Curiously, the peptide mass for the HNE-modified peptide that would be predicted to contain the HNE−Cys-149 adduct (i.e., Ile-143 − Lys-159 + 156 Da = 1859 Da) was not found. In addition, the unmodified peptide encompassing Cys-149 (i.e., peak 31 consisting of Ile-143 − Lys-159 with a molecular mass of 1703.5 Da) is found without any modification. We indeed measured the relative ion abundances of the unmodified peptide as a function of HNE reaction time and found that they were constant during incubations: 1.39×10^7 at 0 min, 1.54×10^7 at 5 min, 2.21×10^7 at 15 min, and 1.20×10^7 at 30 min. These observations suggest that the catalytic center Cys-149 does not undergo HNE modification. Figure 7 shows the location of the target amino acids on the GAPDH molecule, indicating that HNE inactivation of GAPDH is not due to the modification of the catalytic site but to the selective modification of the amino acids primarily located in the surface of the GAPDH molecule.

DISCUSSION

A variety of enzymes have been shown to be susceptible to inactivation from the HNE active site adducts, including the glucose-6-phosphate dehydrogenase (*12*), glutathione *S*-transferase (*22*), glutathione reductase (*23*), interleukin 1B converting enzyme (*24*), and aldose reductase (*25*). These studies used a variety of tools to assess HNE adduct formation, including quantification of the thioether linkages between the HNE and thiols using Raney nickel (*16*, *26*) and immunochemical detection with anti-HNE antibodies (*27*). Despite much information about the inactivation of enzymes by HNE (*3*), a detailed mechanism of the HNE modification of enzymes had rarely been characterized. However, a recent mass spectrometry approach, using ESI-LC−MS and MALDI-TOF MS, has permitted the direct identification of the modification sites in the enzymes. Crabb *et al*. (*28*) demonstrated that, by using a combination of immunochemical and mass spectrometric methods, HNE

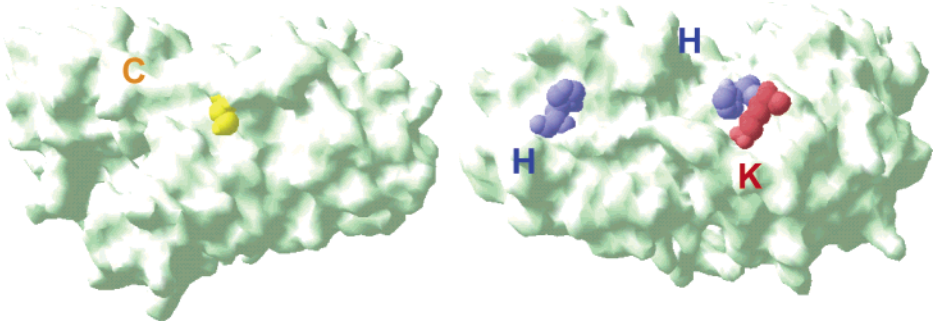

FIGURE 7: Formation of HNE Michael adducts in GAPDH. The structure of the rabbit muscle GAPDH is shown with the cysteine, histidine, and lysine residues that are modified by HNE at 30 min. The structure was drawn using swis-PdbViewer version 3.7b2 (ExPASy Molecular Biology Server), and the PDB coordinates for rabbit GAPDH (AAAa0LY2A) were obtained from an automated comparative protein modeling server (SWISS-MODEL in ExPASy Molecular Biology Server).

treatment of the purified bovine cathepsin B results in selective modification of active site residues, Cys-29 (A chain) and His-150 (B chain), with the generation of Michael adducts and significantly reduced enzyme activity. Musatov *et al*. (*29*) identified a bovine heart cytochrome *c* oxidase subunit, subunit VIII, which is modified more than any other subunit by HNE, and identified His-36 as the HNE-modified amino acid residue within subunit VIII by tandem mass analysis.

In the study presented here, we investigated the covalent binding of HNE to GAPDH during the early stage within 30 min of incubation. We observed that, upon incubation of GAPDH (1 mg/mL) with 1 mM HNE for 30 min, the enzyme activity linearly declined to 50% of the initial value (Figure 2A) and that the loss in activity was accompanied by the loss of three amino acid residues, cysteine (sulfhydryl groups), lysine, and histidine (Figure 2B). It is evident that the loss of catalytic activity is correlated with the loss of these amino acids after incubation for 15 min, where 2 cysteine, 1 histidine, and 0.2 lysine residues per subunit were lost and 30% of the catalytic activity was lost. The loss of enzyme activity and modification of the histidine and lysine continued with further incubation, while the modification of the cysteine was nearly complete. The 30 min treatment with HNE modified 2 cysteine, 1.3 histidine, and 0.5 lysine residues per subunit (Figure 2B). Covalent binding of HNE to these amino acids was also confirmed by the protein carbonyl assay (Figure 2C), by the immnuoblot analysis using the anti-HNE−histidine monoclonal antibody (Figure 2D), and by MALDI-TOF MS analysis (Figure 3), providing strong evidence that the reaction between HNE and GAPDH primarily occurred *via* the Michael addition reaction.

GAPDH, an important enzyme, which catalyzes the oxidation and phosphorylation of D-glyceraldehyde 3-phosphate to 1,3-diphosphoglycerate, is a tetrameric enzyme consisting of four identical catalytically active subunits. Each subunit has four cysteine residues, of which Cys-149 is at the active site. This cysteine is involved in the catalysis and is highly reactive (*30*). Alkylation of this cysteine residue by agents such as iodoacetate or iodoacetamide has been shown to lead to irreversible inhibition of enzyme activity and, therefore, glycolytic ATP synthesis (*30*). In addition to Cys-149, Cys-153 has also been suggested to be sensitive to oxidizing agents (*31*). Comparative studies on the primary structures of GAPDH from different species of animals have shown that the amino acid sequence around the active site cysteine residue is highly conservative over a range of 12 amino acids (*32*, *33*). This invariant sequence is Ser-Asn-Ala-Ser-Cys*-149-Thr-Thr-Asn-Cys-153-Leu-Ala-Pro. Cys-153 is very close to the active site Cys-149 and is also one of the evolutionally conservative amino acids. Thus, Cys-153 also seems to be important for enzyme activity. However, the target of HNE in GAPDH was not either Cys-149 or Cys-153, but the targets were the other two cysteine residues, Cys-244 and Cys-281, outside the active center. In addition, as the target amino acids, we identified other three amino acids, His-164, His-327, and Lys-331, located in the surface of the protein molecule (Figure 7). Among these five target amino acids, both Cys-281 and His-164 most rapidly underwent HNE modification. Whether both Cys-281 and His-164 are modified in the same GAPDH molecule is not clear as unmodified peptides containing these residues were detected in the LC−MS analysis (Figure 4). Therefore, the HNE modification of Cys-281 and/or His-164 would disrupt the enzyme reaction mechanism. On the basis of the reactivity of HNE toward sulfhydryl groups, we speculate that HNE first reacts with Cys-281, rendering His-164 also susceptible to electrophilic attack by HNE. Such a mechanism of selective HNE modification could have an impact on the activity of the thiol enzymes in an oxidative stress environment. On the basis of the observations that the alkylation of Cys-281 causes a rapid and complete precipitation of the protein whereas, as a control, the yeast enzyme, which does not contain a cysteine at position 281, cannot be precipitated under the alkylation conditions, it has been suggested that one of the earliest targets, Cys-281, plays an important role in the maintenance of the GAPDH structure (*34*). The significance of covalent modification of other amino acids, Cys-244, His-327, and Lys-331, on GAPDH function and/or structure remains unknown.

It should be noted that the key active site peptide, having a theoretical molecular mass of 1706.0 Da, gave an average molecular mass of 1703.5 Da (peak 31 in Table 1). The loss of 2 Da might be due to the formation of a disulfide bond between Cys-149 and Cys-153. Because Cys-149 represents the active site of the enzyme, formation of the disulfide bond between two cysteine residues should directly lead to the inactivation of the enzyme. However, no detectable decrease in enzyme activity was observed during incubation of the enzyme alone (E. Tatsuda, T. Ishii, and K. Uchida, unpublished observation), suggesting that the disulfide bond might be formed during proteolysis and/or LC−MS.

GAPDH is a sensitive enzyme in oxidant-mediated cell injury (*35*). In addition, GAPDH is known to be potentially

modified by many other processes, including S-glutathiolation (*36*, *37*) and S-nitrosylation (*38*), both of which decrease its activity in response to some form of stress. We have previously shown that cells exposed to HNE resulted in the partial loss of cellular GAPDH activity (*17*). The inhibition of GAPDH may represent the metabolic perturbation during glycolysis. Therefore, this study suggests a possible contribution of impaired energy homeostasis during HNE-mediated cellular injury to the process of cell dysfunction and cell death. In addition to its role as a glycolytic enzyme, the HNE modification of GAPDH followed by its inactivation may seriously affect other cellular functions because GAPDH is known to take part in a broad array of biological activities: (i) regulation of microtubule bundling (*39*), (ii) binding to erythroid cell membranes (*40*), (iii) muscle triad junction formation (*41*), (iv) function as a protein kinase (*42*) and a uracil DNA glycosylase (*43*), and (v) and RNA nuclear export (*44*).

Time-resolved alkylation studies with mass spectrometry readouts have been carried out previously (e.g., protein folding work with cysteine alkylation to map disulfide bond formation during protein refolding) (*45*). The alkylated structure of various intermediates determined in a time course manner should provide clues to the alkylation pathway of protein in the particular medium. In this study, we characterized the time-resolved HNE modification of GAPDH by LC−MS and identified five peptides, which contained the HNE Michael adducts at His-164, Cys-244, Cys-281, His-327, and Lys-331. We also revealed that the catalytic center Cys-149 did not undergo HNE modification. These data suggest that the HNE inactivation of GAPDH is due not to the modification of the catalytic center but to the selective modification of the amino acids primarily located in the surface of the GAPDH molecule.

ACKNOWLEDGMENT

We thank Dr. Sakai (University of Shizuoka) for his helpful advice and M. Ohkura (University of Shizuoka) for technical assistance.

REFERENCES

1. Shacter, E. (2000) *Drug Metab. Rev. 32*, 307−326.
2. Stadtman, E. R., and Levine, R. L. (2000) *Ann. N.Y. Acad. Sci. 899*, 191−208.
3. Esterbauer, H., Schaur, R. J., and Zollner, H. (1991) *Free Radical Biol. Med. 11*, 81−128.
4. Uchida, K. (2000) *Free Radical Biol. Med. 28*, 1685−1696.
5. Steinberg, D., Parthasarathy, S., Carew, T. E., Khoo, J. C., and Witztum, J. L. (1989) *N. Engl. J. Med. 320*, 915−924.
6. Steinberg, D. (1995) *Adv. Exp. Med. Biol. 369*, 39−48.
7. Benedetti, A., Comporti, M., and Esterbauer, H. (1980) *Biochim. Biophys. Acta 620*, 281−296.
8. Benedetti, A., Pompella, A., Fulceri, R., Ramani, A., and Comporti, M. (1986) *Biochim. Biophys. Acta 876*, 658−666.
9. Esterbauer, H., Zollner, H., and Scholz, N. (1975) *Z. Naturforsch. c30*, 466−473.
10. Schauenstein, E., and Esterbauer, H. (1979) *Ciba Found. Symp. 67*, 225−244.
11. Uchida, K., and Stadtman, E. R. (1992) *Proc. Natl. Acad. Sci. U.S.A. 89*, 4544−4548.
12. Szweda, L. I., Uchida, K., Tsai, L., and Stadtman, E. R. (1993) *J. Biol. Chem. 268*, 3342−3347.
13. Brodie, A. E., and Reed, D. J. (1987) *Biochem. Biophys. Res. Commun. 148*, 120−125.
14. Brodie, A. E., and Reed, D. J. (1990) *Arch. Biochem. Biophys. 276*, 212−218.
15. Ashida, H., and Kanazawa, K. (1991) *Arch. Biochem. Biophys. 288*, 71−78.
16. Uchida, K., and Stadtman, E. R. (1993) *J. Biol. Chem. 268*, 6388−6393.
17. Fukuda, A., Osawa, T., Hitomi, K., and Uchida, K. (1996) *Arch. Biochem. Biophys. 333*, 419−426.
18. De Montarby, L., Mosset, P., and Gree, R. (1988) *Tetrahedron Lett. 29*, 3895.
19. Toyokuni, S., Miyake, N., Hiai, H., Hagiwara, M., Kawakishi, S., Osawa, T., and Uchida, K. (1995) *FEBS Lett. 359*, 189−191.
20. Levine, R. L., Williams, J. A., Stadtman, E. R., and Shacter, E. (1994) *Methods Enzymol. 233*, 346−357.
21. Laemmli, U. K. (1970) *Nature 227*, 680−685.
22. Mitchell, A. E., Morin, D., Lame, M. W., and Jones, A. D. (1995) *Chem. Res. Toxicol. 8*, 1054−1062.
23. Vander Jagt, D. L., Hunsaker, L. A., Vander Jagt, T. J., Gomez, M. S., Gonzales, D. M., Deck, L. M., and Royer, R. E. (1997) *Biochem. Pharmacol. 53*, 1133−1140.
24. Davis, D. W., Hamilton, R. F., and Holian, A. (1997) *J. Interferon Cytokine Res. 17*, 205−219.
25. Del Corso, A., Dal Monte, M., Vilardo, P. G., Cecconi, I., Moschini, R., Banditelli, S., Cappiello, M., Tsai, L., and Mura, U. (1998) *Arch. Biochem. Biophys. 350*, 245−248.
26. Uchida, K., and Stadtman, E. R. (1992b) *Proc. Natl. Acad. Sci. U.S.A. 89*, 5611−5615.
27. Uchida, K., Szweda, L. I., Chae, H. Z., and Stadtman, E. R. (1993) *Proc. Natl. Acad. Sci. U.S.A. 90*, 8742−8746.
28. Crabb, J. W., O'Neil, J., Miyagi, M., West, K., and Hoff, H. F. (2002) *Protein Sci. 11*, 831−840.
29. Musatov, A., Carroll, C. A., Liu, Y. C., Henderson, G. I., Weintraub, S. T., and Robinson, N. C. (2002) *Biochemistry 41*, 8212−8220.
30. Harris, J. L., and Walters, M. (1976) in *Glyceraldehyde-3-phosphate dehydrogenase* (Boyer, P. D., Ed.) p 19, The Enzymes, Academic Press, New York.
31. Wassarman, P. M., and Major, J. P. (1969) *Biochemistry 8*, 1076−1082.
32. Perham, R. N., and Harris, J. I. (1963) *J. Mol. Biol. 7*, 316−320.
33. Allison, W. S. (1968) *Ann. N.Y. Acad. Sci. 148*, 180−189.
34. Bond, J. S., Francis, S. H., and Park, J. H. (1970) *J. Biol. Chem. 245*, 1041−1053.
35. Hyslop, P. A., Hinshaw, D. B., Halsey, W. A., Schraufstätter, I. U., Sauerheber, R. D., Spragg, R. G., Jackson, J. H., and Cochrane, C. G. (1988) *J. Biol. Chem. 263*, 1665−1675.
36. Schuppe-Koistinen, I., Moldéus, P., Bergman, T., and Cotgreave, I. A. (1994) *Eur. J. Biochem. 221*, 1033−1037.
37. Ravichandran, V., Seres, T., Moriguchi, T., Thomas, J. A., and Johnston, R. B., Jr. (1994) *J. Biol. Chem. 269*, 25010−25015.
38. Mohr, S., Stamler, J. S., and Brüne, B. (1996) *J. Biol. Chem. 271*, 4209−4214.
39. Huitorel, P., and Pantaloni, D. (1985) *Eur. J. Biochem. 150*, 265−269.
40. Allen, R. W., Trach, K. A., and Hoch, J. A. (1987) *J. Biol. Chem. 262*, 649−653.
41. Caswell, A. H., and Corbett, A. M. (1986) *J. Biol. Chem. 260*, 6892−6898.
42. Kawamoto, R. M., and Caswell, A. H. (1986) *Biochemistry 25*, 656−661.
43. Meyer-Siegler, K., Mauro, D. J., Seal, G., Wurzer, J., DeRiel, J. K., and Sirover, M. A. (1991) *Proc. Natl. Acad. Sci. U.S.A. 88*, 8460−8464.
44. Singh, R., and Green, M. R. (1993) *Science 259*, 365−368.
45. Watson, J. T., Yang, Y., and Wu, J. (2001) *J. Mol. Graphics Modell. 19*, 119−128.

BI027172O